

Polyacrylamide Gel Photopatterning Enables Automated Protein Immunoblotting in a Two-Dimensional Microdevice

Mei He and Amy E. Herr*

Department of Bioengineering, University of California, Berkeley, California 94720

Received December 2, 2009; E-mail: aeh@berkeley.edu

Immunoblotting has revolutionized the life sciences and important aspects of diagnostic medicine.¹ Protein immunoblotting is central to studies ranging from cellular signaling to confirmatory serum diagnosis of HIV.² In 1979 Towbin and colleagues introduced the multistage immunoblotting assay (i.e., Western blotting) to overcome the challenge of spurious binding of fluorescently labeled antibody probes to nontarget proteinaceous sample components, as can occur in immunohistochemistry and flow cytometry.³ To achieve high-specificity protein identification in a single assay, protein immunoblotting reports analyte identity by sequentially assaying two characteristics: (i) protein electrophoretic mobility (μ , e.g., charge to mass ratio, size or molecular weight) and (ii) binding between resolved protein target and antibody probe. The unrivaled specificity of immunoblotting arises from this capability to directly map analyte mobility to the presence or absence of an antibody-binding interaction.

While powerful and ubiquitous, conventional slab-gel immunoblotting has numerous drawbacks, yet the approach has changed little since introduction. The technique suffers from a manual, low-throughput nature—often requiring days to complete and necessitating interventions by a skilled operator. Slab-gel electrophoresis, the first step, requires hours. The second step, protein transfer to the membrane, is also time consuming and suffers from variable blotting efficiency and reproducibility.⁴ Large molecular weight species are notoriously difficult to transfer.⁵ The last step, blotting with antibodies, requires an incubation step and consumes substantial antibody mass ($\sim 10 \mu\text{g}$), which is especially detrimental as antibodies are typically costly and vary in affinity from lot-to-lot.⁶

To overcome the noted limitations, we have designed, fabricated, and validated an automated immunoblotting assay that relies on high-resolution polyacrylamide (PA) gel photopatterning in a two-dimensional (2D) microfluidic architecture to yield polyacrylamide gel electrophoresis (PAGE), transfer, and antibody-functionalized blotting regions (Figure 1, and Figures S1, S2 and Table S1 in Supporting Information (SI)). To our knowledge, limited effort has been made to streamline the multiple steps needed to obtain mobility and binding-based identity information in one continuous assay.⁷ Though similar 2D channel networks have yielded notable performance for free-flow electrophoresis and nanostructured sieving assays,^{8–10} we use a chamber patterned with various PA gels to mimic both a miniature slab gel and a protein-binding membrane. Importantly, our chip design enables blotting of all protein bands from PAGE against the blotting region in a single electrophoretic transfer step that is fully programmable.

The reported performance is an important improvement over our previous work,¹¹ as the gel chamber allows direct mapping of protein mobility to antibody binding using full-field imaging. Through simulation and empirical adjustment of the applied potentials and optimization of the gel architecture, we achieve high performance in all three transport processes core to immunoblotting:

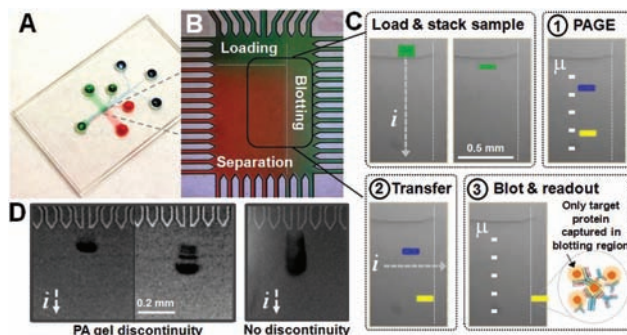


Figure 1. Polyacrylamide gel photopatterning in a 2D microfluidic geometry enables fully integrated protein immunoblotting. Bright-field images of: (A) glass device housing patterned PA gels and (B) magnified chamber with photopatterned gels for sample loading (blue), PAGE separation (red) and transfer to antibody functionalized blotting region (green). (C) The automated multistage assay protocol is overlaid on micrographs of the microdevice. (D) Large-to-small pore size discontinuity at PAGE start yields size-based PSA sample stacking (inverted grayscale). μ is mobility; “ i ” indicates direction of electrical current flow.

separation, sample transfer, and antibody-based blotting (Figure S3 in SI). To optimize the first step (PAGE), we use a discontinuous gel (large-to-small pore size) near the sample injector to minimize injection dispersion for improved separation resolution (SR). Using the gel discontinuity, PAGE achieves an $SR = 1.5$ for the two highest mobility peaks in Figure 1D, whereas without the discontinuity, $SR = 0.4$ for the same two species.

We implemented a complete native immunoblot of free prostate specific antigen (fPSA) extracted from human seminal fluid (Figure 2). Free PSA is a tumor marker currently used for serum diagnosis of prostate cancer. Much recent interest centers on improving prognostic performance through analysis of other forms of PSA and alternate diagnostic fluids (nonserum).¹² Using our microfluidic immunoblot, native PAGE analysis completed within 36 s with an average $SR = 1.59$ (pairwise for labeled proteins in Figure 2, detailed in Table S2 in SI). After PAGE, the on-chip transfer step required 30–60 s, compared with 2 h in slab-gel systems (Table 1). A major consideration in the transfer step is conservation of SR and mobility information. During the transfer, electric field shaping and use of PA gels yielded a transfer efficiency of $\sim 90\%$ (Figure S4B in SI) and an SR loss of 6% (Table S2 in SI). Large and small molecular weight species were efficiently transferred, with no sample retained along the separation or transfer axes.

In the blotting stage, species exhibiting affinity for the blotting membrane were retained in the blotting region, while species with low-to-no affinity freely migrated past the blotting region, as shown for the three non-fPSA proteins in the sample (Figure 2). Several non-fPSA peaks were also detected by slab-gel electrophoresis under native and 12% SDS conditions with postseparation staining (Figure S4A in SI). The target fPSA protein was identified by on-

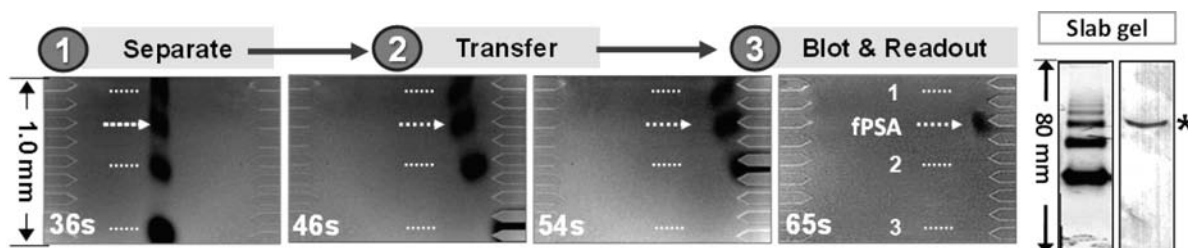


Figure 2. On-chip immunoblotting of native fPSA extracted from human seminal fluid is rapid and automated. Fluorescence CCD images show the PA gel patterned chamber during: separation, transfer, and blot. A conventional native slab mini-gel blot allows comparison (inverted grayscale, * marks fPSA, numerals 1–3 mark non-fPSA sample peaks).

chip immunoblotting with immobilized anti-fPSA antibody ($\sim 1 \mu\text{g}$) in 65 s. A signal-to-noise ratio of 40 was detected for fPSA (500 nM) in the blotting region. Further detection sensitivity optimization is underway. The on-chip fPSA immunoblotting result was confirmed with conventional native slab mini-gel blotting, which required 2 days to complete (Figure S4A in SI, Table 1).

Table 1. On-Chip vs Slab Mini-Gel Immunoblotting of PSA Sample

		on-chip	conventional WB ⁶
Transfer	reproducibility	3%	15% ¹³
	SR loss	6%	15% ¹⁴
	efficiency	90%	67.8% ⁴
Duration	separation	30–60 s	2 h
	transfer	30 s	2 h
	blotting	30 s	6–8 h

To further assess the versatility of the PAGE-transfer sequence, we considered two additional PAGE systems: sodium dodecyl sulfate (SDS) and cetyl trimethylammonium bromide (CTAB) (Figure S5, SI). As expected for sizing assays, the log molecular weight was linearly related to protein mobility with $R_{\text{SDS}}^2 = 0.96$ and $R_{\text{CTAB}}^2 = 0.90$, comparable to slab-gel SDS-PAGE ($R^2 = 0.98$). A $\sim 2.5\%$ migration reproducibility was obtained for on-chip sizing PAGE ($n = 4$) (Figure S5B, SI). Transfer of the resolved proteins from the PAGE separation to the blotting region resulted in $<10\%$ loss in SR and $<4\%$ band shifting, indicating satisfactory conservation of mobility information during the transfer step (Table S3, SI). As compared to slab mini-gel PAGE, on-chip PAGE was completed in 4% of the separation length and in 0.5% of the time, with improved transfer efficiency.

We have introduced a facile, rapid immunoblotting assay that utilizes a single microfluidic chamber photopatterned with heterogeneous gel elements to unify PAGE protein separation, electrophoretic transfer, and antibody-based in-gel blotting. Mapping of the separation axis to the blotting region yields both electrophoretic mobility and binding information. As demonstrated, the native immunoblot for fPSA required fewer than 5 min to complete. Inclusion of a gel pore size discontinuity at PAGE start minimized injection dispersion in the chamber.

The directed transfer of proteins from the separation to the blotting region was also low-dispersion and benefited from both

microfluidic scaling (i.e., short transfer distance) and integration. This programmable assay affords ‘walk-away’ operation. Further, antibody-patterning of the blotting region by the end-user consumes limited blotting antibodies and allows assay customization even after device fabrication and storage, as demonstrated in our previous work¹¹ and relevant to the 2D geometry presented here. The heterogeneous gel approach introduced is a powerful new tool applicable to a broad range of multistage assays, including DNA/RNA blotting and multidimensional separation strategies. We are further developing the approach for analysis of complex protein samples relevant to both basic science and clinical questions.

Acknowledgment. We gratefully acknowledge Prof. D. Peehl (Stanford) for the PSA sample, as well as Dr. Yong Zeng and Mr. Samuel Tia for assistance. We thank the University of California, Berkeley, the QB3/Rogers Family Foundation Award, and UC Berkeley NSF COINS for financial support.

Supporting Information Available: Detailed experimental procedures regarding the device fabrication and operation, electric field shaping optimization, conventional immunoblotting results, and complete refs 7 and 12. This material is available free of charge via the Internet at <http://pubs.acs.org>.

References

- (1) Tissot, J. D.; Vu, D. H.; Aubert, V.; Schneider, P.; Vuadens, F.; Crettaz, D.; Duchosal, M. A. *Proteomics* **2002**, *2*, 813–824.
- (2) Gershoni, J. M.; Palade, G. E. *Anal. Biochem.* **1983**, *131*, 1–15.
- (3) Towbin, H.; Staehelin, T.; Gordon, J. *Proc. Natl. Acad. Sci. U.S.A.* **1979**, *76*, 4350–4354.
- (4) Jungblut, P.; Eckerskorn, C.; Lottspeich, F.; Klose, J. *Electrophoresis* **1990**, *11*, 581–588.
- (5) Kurien, B. T.; Scofield, R. H. *J. Immunol. Meth.* **2002**, *266*, 127–133.
- (6) Wu, Y.; Li, Q.; Chen, X. Z. *Nat. Protoc.* **2007**, *2*, 3278–3284.
- (7) O’Neill, R. A.; et al. *Proc. Natl. Acad. Sci. U.S.A.* **2006**, *103*, 16153–16158.
- (8) Zeng, Y.; He, M.; Harrison, D. J. *Angew. Chem., Int. Ed.* **2008**, *47*, 6388–6391.
- (9) Huang, L. R.; Tegenfeldt, J. O.; Kraeft, J. J.; Sturm, J. C.; Austin, R. H.; Cox, E. C. *Tech. Dig. Int. Electron Devices Meet.* **2001**, 363–366.
- (10) Yamada, M.; Mao, P.; Fu, J.; Han, J. *Anal. Chem.* **2009**, *81*, 7067–7074.
- (11) He, M.; Herr, A. E. *Anal. Chem.* **2009**, *81*, 8177–8184.
- (12) Andriole, G. L.; et al. *New Engl. J. Med.* **2009**, *360*, 1310–1319.
- (13) Ochoa, M. T.; Fhølenhag, K.; Malmlöf, K.; Sánchez-Gómez, M.; Skottner, A. *Arch. Latinoam. Nutr.* **1997**, *47*, 331–337.
- (14) Cowan, S. L.; Diem, L.; Brake, M. C.; Crawford, J. T. *J. Clin. Microbiol.* **2004**, *42*, 474–477.

JA910164D